



OPEN ACCESS

EDITED BY

Nan Wu,
Tongji University, China

REVIEWED BY

Yuan Li,
Hubei Earthquake Administration, China
Qiangtai Huang,
Sun Yat-sen University, China

*CORRESPONDENCE

Entao Liu

✉ liuentao@cug.edu.cn

Detian Yan

✉ yandetian@cug.edu.cn

RECEIVED 21 August 2023

ACCEPTED 23 October 2023

PUBLISHED 23 November 2023

CITATION

Liu E, Yan D, Pei J, Lin X and Zhang J
(2023) Sedimentary architecture and
evolution of a Quaternary sand-rich
submarine fan in the South China Sea.
Front. Mar. Sci. 10:1280763.
doi: 10.3389/fmars.2023.1280763

COPYRIGHT

© 2023 Liu, Yan, Pei, Lin and Zhang. This is an open-access article distributed under the terms of the [Creative Commons Attribution License \(CC BY\)](https://creativecommons.org/licenses/by/4.0/). The use, distribution or reproduction in other forums is permitted, provided the original author(s) and the copyright owner(s) are credited and that the original publication in this journal is cited, in accordance with accepted academic practice. No use, distribution or reproduction is permitted which does not comply with these terms.

Sedimentary architecture and evolution of a Quaternary sand-rich submarine fan in the South China Sea

Entao Liu^{1,2*}, Detian Yan^{3*}, Jianxiang Pei^{3,4}, Xudong Lin¹
and Junfeng Zhang³

¹Hubei Key Laboratory of Marine Geological Resources, China University of Geosciences, Wuhan, China, ²Radiogenic Isotope Facility, School of Earth and Environmental Sciences, The University of Queensland, Brisbane, QLD, Australia, ³Key Laboratory of Tectonics and Petroleum Resources, Ministry of Education, China University of Geosciences, Wuhan, China, ⁴Hainan Branch Company, China National Offshore Oil Corporation, Haikou, China

Investigating the sedimentary architecture and evolution of sand-rich submarine fans is vital for comprehending deep-water sedimentary processes and enhancing the success rate of hydrocarbon resource exploration. Recent drilling activities in the Qiongdongnan Basin, northern South China Sea, have unveiled significant gas hydrate and shallow gas potential. However, exploration in this area faces substantial challenges due to the limited understanding of sandy reservoirs. Leveraging extensive newly acquired extensive 3D seismic data (~9000 km²) and well data, our study reveals five distinct deep-water depositional systems in the Quaternary Ledong Formation, including a submarine fan system, mass transport deposits, deepwater channel-levee systems, slope fans, and hemipelagic sediments. Notably, the targeted sand-rich submarine fan lies within the abyssal plain, situated at a water depth of 1300–1700 m. This fan exhibits a unique tongue-shape configuration and a SW-NE flow direction within the plane and spans an expansive area of ~2800 km² with maximum length and width reaching 140 km and 35 km, respectively. Vertically, the fan comprises five stages of distributary channel-lobe complexes, progressing from Unit 1 to Unit 5. Their distribution ranges steadily increase from Unit 1 to Unit 3, followed by a rapid decrease from Unit 4 to Unit 5. Our results suggest that the occurrence and evolution of the submarine fan are primarily controlled by sea level fluctuation, confined geomorphology, and sediment supply. Specifically, sea level fluctuation and sediment supply influenced the occurrence of the submarine fan. Concurrently, the confined geomorphology in the abyssal plain provided accumulation space for sediments and shaped the fan into its distinct tongue-like form. In contrast to the deepwater channels within the deepwater channel-levee systems, the distributary turbidite channels within the submarine fan are marked by lower erosion depth with “U” shapes, greater channel width, and higher ratios of width to depth. The comparative analysis identifies turbidite channels as the focal points for

offshore gas hydrate and shallow gas exploration in the Qiongdongnan Basin. Furthermore, the temporal evolution of submarine fan offers valuable insights into Quaternary deep-water sedimentary processes and hydrocarbon exploration within shallow strata of marginal ocean basins.

KEYWORDS

submarine fan, sand-rich reservoirs, sedimentary architecture, Quaternary, South China Sea

1 Introduction

Submarine fan systems are formed by sediment gravity flows shed from continental margins into ocean basins and commonly deposited in abyssal plains (Normark, 1970; Piper and Normark, 2001; Talling et al., 2007). These systems have garnered significant attention both economically and academically due to their vast hydrocarbon exploration potential and their importance in hazard assessment (Richard et al., 1998). Over the past few decades, numerous submarine fan systems have been identified and studied, including those in the Gulf of Mexico, the North Sea, offshore West Africa, and the northern South China Sea (Mattern, 2005; Covault et al., 2007; Deptuck et al., 2008). Previous research indicates that submarine fan systems often exhibit considerable variability in depositional characteristics and complex sedimentary architectures, resulting from multiple mechanisms of sediment transport from continental shelf slopes to abyssal plains (Clift and Gaedicke, 2002; Mattern, 2005; Pickering et al., 2015; Sun et al., 2022; Zhang and Hou, 2022). These complexities pose significant challenges for hydrocarbon exploration.

Gas hydrate is considered an efficient and clean energy source, with the majority of recoverable gas hydrate resources concentrated in deep subsea sands (Boswell and Collett, 2011). Shallow gas, on the other hand, is an unconventional energy source enriched within shallow strata, typically located at depths less than 1000 m below the seafloor. This shallow gas is commonly found in the lower strata of gas hydrate reservoirs (Horozal et al., 2009). Submarine fans are known to house some of the largest gas hydrate and shallow gas reservoirs due to their higher permeability and porosity when compared to other sedimentary facies, such as mass-flow deposits (Mattern, 2005; Portnova et al., 2019; Liu et al., 2020; Liu et al., 2021; Liu et al., 2023). For instance, in the Nankai Trough, gas hydrate reservoirs are primarily composed of turbidite sands, hosting hydrate mainly within the primary pore space of these sands (Uchida and Tsuji, 2004; Collett et al., 2012). Similarly, high concentrations of gas hydrate in the Gulf of Mexico are found in sand-rich submarine fan turbidities, with saturations reaching up to 75% (Boswell et al., 2009; Portnova et al., 2019). Consequently, exploring the sedimentary architecture and evolution process of sand-rich submarine fans in Quaternary strata can not only offer valuable insights into the deepwater sedimentary processes of continental margins but also assist in guiding the exploration of gas hydrate and shallow gas resources.

The study region Qiongdongnan Basin is one of the largest regions for hydrocarbon exploration in the northern South China Sea. Previous research on natural gas exploration has mainly focused on the deep-buried strata of Yinggehai and Huangliu Formations with buried depths of 1200–3600 m below the seafloor (Yuan et al., 2009; Gong et al., 2011; Gong et al., 2019; Liu et al., 2022). However, in 2018, a complex gas hydrate system was first discovered in the central Qiongdongnan Basin, making it become a hotspot for expanding exploration of gas hydrate and shallow gas. A subsequent gas hydrate expedition in 2019 revealed that sand layers located in the abyssal plain are particularly favorable targets, with an average saturation of 52% (Lai et al., 2021; Cheng et al., 2022; Meng et al., 2022). Unfortunately, the previous studies in the Qiongdongnan Basin mainly focus on the central channel in Early Pliocene (Gong et al., 2011; Huang et al., 2016; Xiong et al., 2021) with less attention given to the Quaternary submarine fan system (Yuan et al., 2009). Meng et al. (2022) and Cheng et al. (2022) have documented that turbidite channels are high-quality gas hydrate reservoirs with high saturation based on very limited 3D seismic data (less than 1000 km²) and drilling cores. By contrast, Liu et al. (2023) suggested that gas hydrates are enriched in a Quaternary submarine fan. However, due to the lack of complete coverage of 3D seismic data, the sedimentary architecture of this submarine fan remains unclear. Additionally, it is worth noting that a systematic seismic sedimentological analysis is essential for this study. Therefore, the first objective of this study is to investigate the sedimentary architecture of the submarine fan system using seismic sedimentology, based on newly acquired 3D seismic data covering an area of approximately 9000 km².

The second aim of this study is to determine the evolution process and controlling factors of the submarine fan. The stratigraphic record and evolution of submarine fans are controlled by many factors including sea level, tectonic, climate, geomorphology, and sediment supply (Mattern, 2005; Deptuck et al., 2008; Brooks et al., 2018). These factors contribute to variations in the available accommodation space and sediment supply routing, ultimately resulting in large-scale variations in the shape, size, and characteristics of submarine fans. However, the main controlling factors differ across different depositional settings (Mattern, 2005; Deptuck et al., 2008). For instance, the evolution processes of submarine fans are mostly attributed to sea level fluctuations (Normark et al., 1998; Clift and Gaedicke, 2002; Samuel et al., 2003), whereas some studies suggest that sediment

supply can result in heterogeneity of submarine fans (Piper and Normark, 2001; Hawie et al., 2019). The studied submarine fan deposited in the central Qiongdongnan Basin exhibits a tongue-shaped morphology (Liu et al., 2023), which is significantly different from the fan-like conceptual models of submarine fans (Somme et al., 2009). By utilizing the newly acquired 3D seismic data and drilling cores, this study aims to document the architecture and evolution process of a Quaternary sand-rich submarine fan in the Qiongdongnan Basin and investigate the controlling factors responsible for its deposition.

2 Geological setting

The Qiongdongnan Basin is a NE-trending Cenozoic petroliferous basin located in the northwestern South China Sea (Figure 1). It is bounded by Hainan Island to the north, Yinggehai-Song Hong Basin to the west, Xiasha Uplift to the south, and Pearl River Mouth Basin to the east, and covers a region of $\sim 8 \times 10^4$ km² (Chen et al., 2023) (Figures 1, 2). Currently, the water depth ranges from 300 m to 2750 m with a margin of continental shelf developed (Figure 2). It can be divided into four structural units including the Northern Depression, the Northern Uplift, the Central Depression, and the Southern Uplift. The submarine fan in this study is situated in the Central Depression.

As a typical Cenozoic basin in the South China Sea, the tectonic evolution of the Qiongdongnan Basin can be divided into three stages: (1) a Paleocene period (45 Ma - 23 Ma) of the syn-rifting stage; (2) an early Miocene to Middle Miocene (23 Ma - 11.6 Ma) thermal subsiding stage; and (3) a late Miocene to recent (11.6 Ma - recent) accelerated subsiding stage (Clift and Sun, 2006; Ren et al., 2014; Cheng et al., 2023) (Figure 3). During the tectonic evolution process, the basin has changed from a rift basin into a depression basin with the depositional environment changing from Eocene lacustrine to Oligocene transitional and Miocene to recent marine environment (Ren et al., 2014; Fyhn et al., 2019) (Figure 3). The deposition thickness in the Qiongdongnan Basin reaches up to 15 km, and the developed strata from the Eocene to Quaternary include Eocene Lingtou Formation, Oligocene Yacheng and Lingshui Formations, Miocene Sanya, Meishan and Huangliu Formations, Pliocene Yinggehai Formation and Quaternary Ledong Formation (Figure 3). Since the middle Miocene (11.6 Ma), the basin entered the accelerated subsiding stage, and the continental slope break together with a central canyon formed (Gong et al., 2011; Huang et al., 2016; Wang et al., 2021; Cheng et al., 2023) (Figure 4). The central canyon deposited in the Miocene Huangliu Formation is 520 km long and 15-20 km wide (Gong et al., 2011) (Figure 5).

The Quaternary Ledong Formation (1.8 Ma to present) is dominated by bathyal to abyssal facies deposits including mass

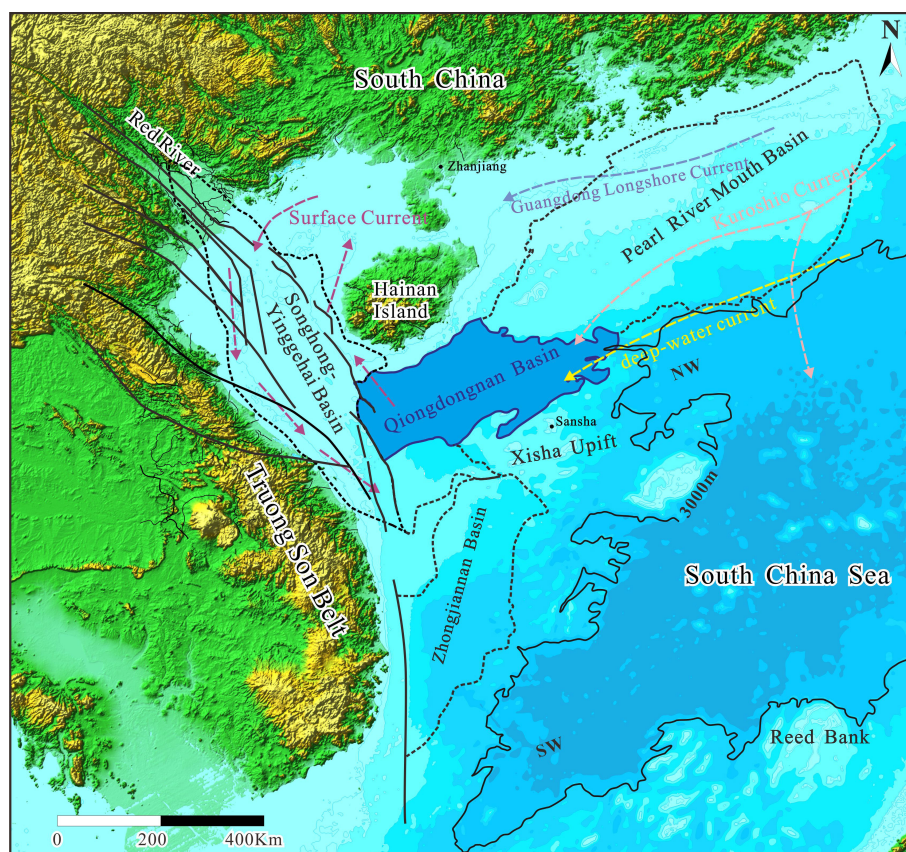


FIGURE 1

The present geomorphic map of the northern continental margin of the South China Sea [modified after Fyhn et al. (2019) and Cheng et al. (2022)], showing the location of the Qiongdongnan Basin. The distribution of currents is from Huang et al. (2023).

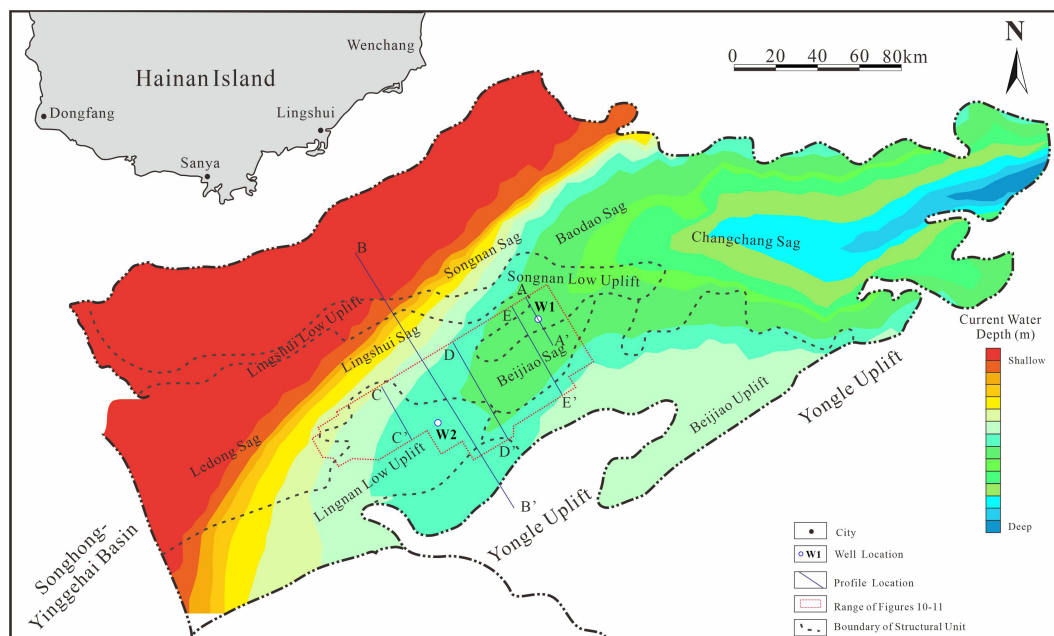


FIGURE 2

The contour map of current water depth and division of tectonic unit in the Qiongdongnan Basin, northern South China Sea (modified after Ren et al. (2022)). The locations of seismic profiles are also shown on the map.

transport deposits, turbidites, a submarine fan system, and pelagic deposits (Cheng et al., 2022; Ren et al., 2022). The studied submarine fan was deposited in the abyssal plain of the central basin with a water depth of 1300–1700 m (Figure 2), and its lithology is represented by unconsolidated silty clays interbedded with sand layers (Ren et al., 2022; Liu et al., 2023). During the sedimentary period of the Ledong Formation, the sedimentation rate is up to 630 m/Ma, but the fault activity rate is extremely low (Ren et al., 2014).

3 Methods

A synergistic approach involving 3D seismic data, well logs, and drilling cores was employed to comprehensively investigate the sedimentary architecture of the submarine fan. The newly-acquired 3D seismic data was provided by the China National Offshore Oil Corporation (CNOOC) in 2023, boasting a peak frequency of approximately 40 Hz. Leveraging the fundamental principles of sequence stratigraphy as elucidated by Catuneanu and Zecchin (2016), a robust temporal stratigraphic framework was meticulously established through the construction of a synthetic seismogram. Geoframe[®] Software was harnessed to meticulously process the seismic data, encompassing an impressive survey area of approximately 9,000 km². Nine sequence boundaries (i.e., T0, S1, S2, S3, S4, S5, S6, S7, and T20) were recognized in well-log and seismic data and were interpreted with the interpretation density of 1 km × 1 km (Figure 4). Following the theory of seismic sedimentology (Zeng, 2013), seismic facies analysis was used to identify the sedimentary architecture and the distribution range of

the submarine fan. Then horizontal coherence slice and root mean square attributes extracted by the Geoframe[®] software were carried out to further constrain the range of the submarine fan and to characterize the depositional microfacies. Using the time-depth conversion formula provided by CNOOC, the palaeogeographic map of Horizon T20 was performed by the Petrel[®] software.

Well 1 and Well 2 were applied to characterize the submarine fan as well. The logging-while-drilling data of Well 1 was obtained from Guangzhou Marine Geological Survey, including natural gamma (GR), acoustic (AC), and resistivity (RES) logging. More than 280 m long continuous chip samples from the newly drilled Well 2 were examined and described to identify the lithologic facies and sedimentary characteristics of the submarine fan.

4 Results

4.1 Seismic-well tie analysis and sequence stratigraphic framework

High-quality natural gamma and acoustic logs from Wells 1 and 2 enabled a seismic-well tie analysis for sequence stratigraphic framework (Figure 5). The seismic-well tie suggests that the Ledong Formation can be divided into eight sedimentation units, and the strata thickness of the Ledong Formation ranges between 230 m and 980 m (Figure 5). The sequence boundary T20 corresponds to 1.8 Ma and is characterized by high-amplitude, moderate-continuity reflections. The internal sequence interfaces within the Ledong Formation (i.e., S1~S7) are marked by either lithologic mutation surfaces or transition surfaces (Figure 5). They

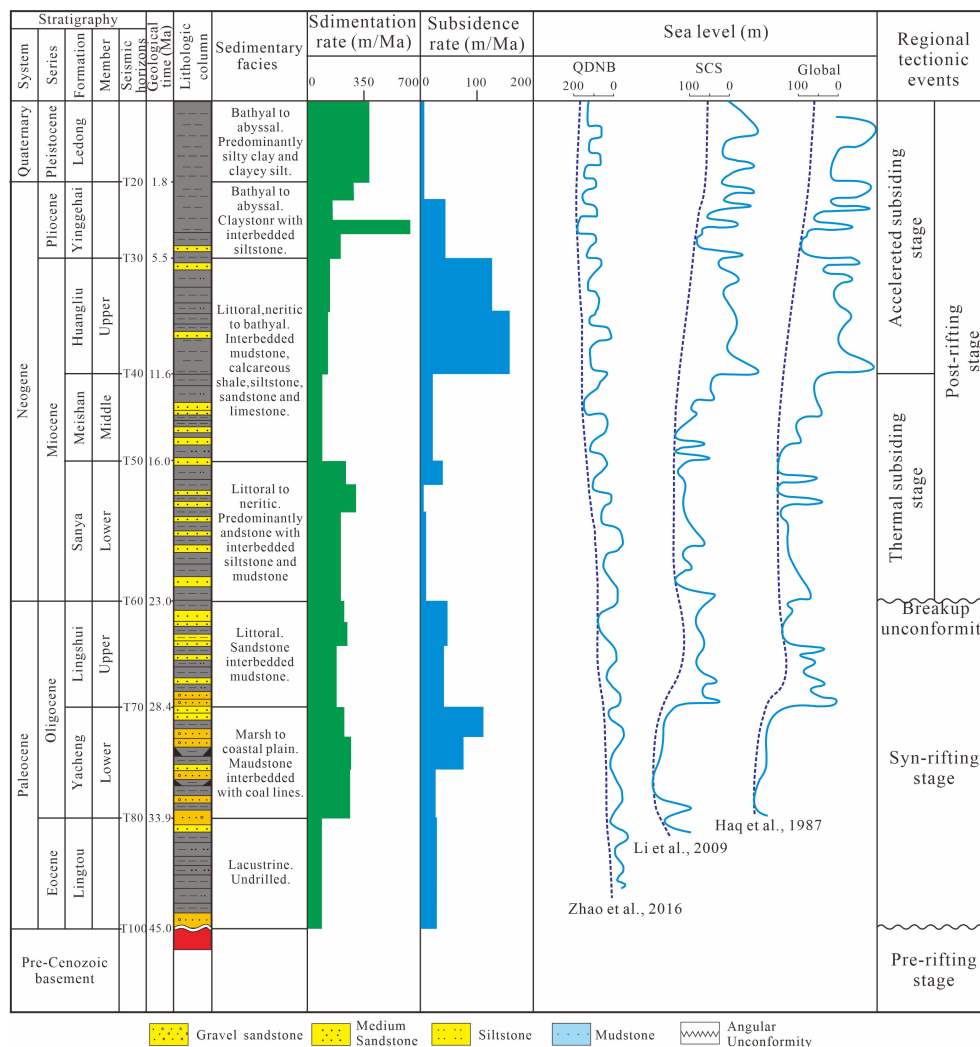


FIGURE 3 Stratigraphic column of the Qiongdongnan Basin, northern South China Sea. The sea level curves are from Haq et al. (1987); Li et al. (2009), and Zhao et al. (2016).

were identified and traced in the 3D seismic data. S1, S2, S3, and S6 are marked by high-amplitude and high-continuity reflections, while S4, S5, and S7 are characterized by high-amplitude and moderate to high-continuity reflections (Figures 6–8). In the abyssal plain of the Qiongdongnan Basin, S1, S2, S3, S4, and S5 surfaces commonly correspond to the boundaries of mass transport deposits (Figures 6–8).

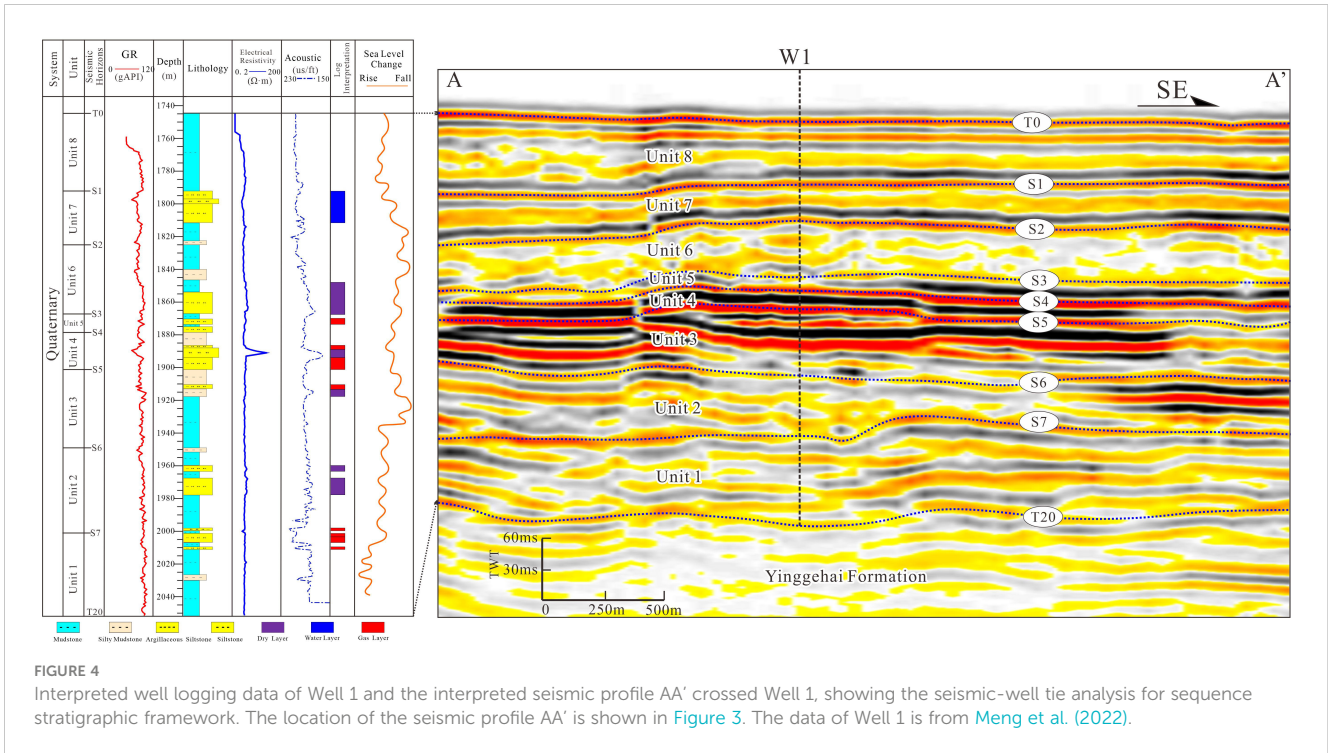
4.2 Seismic facies and corresponding depositional elements

According to the theory of seismic sedimentology (Zeng, 2013), five major seismic facies were identified in the study area, representing different depositional elements including a submarine fan system, mass transport deposits (MTDs), deepwater channel-levee systems, slope fans, and hemipelagic sediments.

4.2.1 Seismic facies 1: submarine fan system

In the seismic profiles, the submarine fan system shows basinward dipping oblique reflectors along the source direction, but lenticular-shaped reflectors perpendicular to the depositional strike (Figures 6–8). Data from Well 2 shows that the submarine fan system is dominated by layered argillaceous siltstone deposits (Figure 9). In RMS attribute images, it is dominated by a large wedge/strip-shaped package with a relatively high amplitude (Figures 10, 11).

Turbidite channel fills are widely developed within the submarine fan system (Figures 10, 11). They have low continuity, low to medium amplitude, and low frequency chaotic seismic reflection characteristics (Figures 6–8). In seismic profiles, they have obvious erosional bases and irregular tops, with erosion depths up to 120 m (average: 26 m), showing U-shaped erosional scours (Figures 6–8). They are dominated by sand-rich sediments with high amplitude in the RMS attribute images (Figures 10, 11).

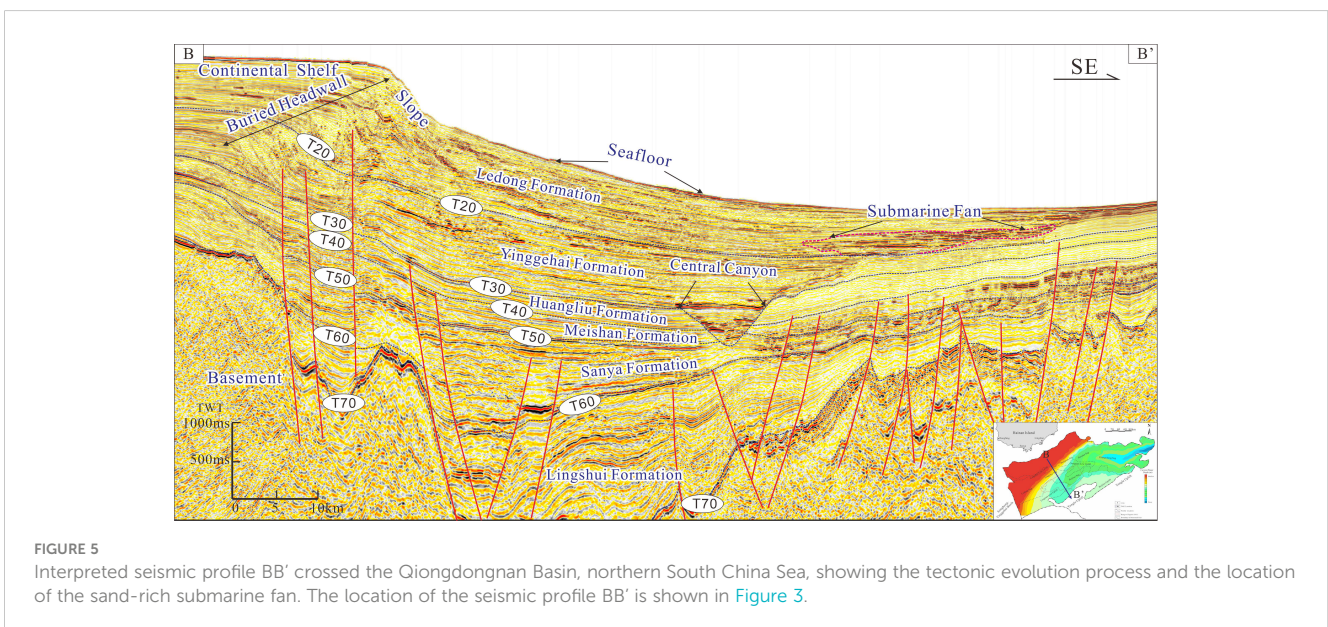


4.2.2 Seismic facies 2: MTDs

MTDs have blank to weak amplitude, low-frequency reflections with sheet-like chaotic or disorganized internal reflection structures (Figures 6–8). In seismic profiles, they can be easily identified by large-scale chaotic seismic reflection patterns (Figures 6–8). They commonly show bottom flattened and top raised strip outlines (Figures 6–8). In the RMS attribute images, MTDs show low amplitude (Figures 10, 11). More than 6 stages of MTDs were recognized in the Ledong Formation, with most of them located above the submarine fan system (Figures 10, 11).

4.2.3 Seismic facies 3: deepwater channel-levee systems

The deepwater channel-levee system shows medium to high-frequency seismic reflections, low to medium continuity with its amplitude intensity decreasing from the channel axis to the flank (Figures 6–8). It is marked by multiple continuous V-shaped erosional surfaces (Figures 6–8). The deepwater channel-levee systems were located in the eastern region with their location varying in different stages (Figures 10, 11). For example, it was away from the submarine fan system during the depositional period



of Unit 1 (Figures 6–8, 10). But it reworked the deposits of the submarine fan with its developed region overlap with the submarine fan during the depositional periods of Units 2–4 (Figures 6–8, 10, 11).

It can be divided into two parts including deepwater channel fill and channel levee (Figures 10, 11). Channel fills represent the channel axial deposits, while channel levees are located on the west flanks of the channel files (Figures 10, 11). Channel levees have the characteristics of continuous reflectors, low-angle imbricated progradation patterns, and gull-wing shapes (Figures 6–8). Multiple deepwater channel-levee systems have been recognized in the study regions and the thickness of a single channel is 0.5–2 km in width and more than 200 km in length (Figures 6–8). The channel levees are 5–15 km in width, displaying wedge shapes (Figures 10, 11).

4.2.4 Seismic facies 4: slope fans

Seismic facies 4 shows progradational seismic reflection patterns with medium to high continuity and medium to high amplitude in seismic profiles (Figures 6–8). In the RMS attribute images, slope fans show relatively high attributes (Figures 10, 11). Moreover, slope fans can be distinguished from the submarine fan by the developmental site. For details, the submarine fan was located in the abyssal plain, while slope fans were situated close to the continental shelf break (Figures 10, 11).

4.2.5 Seismic facies 5: hemipelagic sediments

Seismic facies 5 shows low amplitude, high-continuity reflectors with a parallel, sheet-like configuration (Figures 6–8). It consists of thick-bedded mudstone, indicating hemipelagic sediments in the deep-water setting.

4.3 Distribution and sedimentary architecture of the submarine fan

Based on the above sedimentological and sequence stratigraphy analysis, the studied submarine fan can be divided into five stages of

distributary channel-lobe complexes from Unit 1 to Unit 5 (Figures 10, 11).

Unit 1 sedimentary period: The distributary channel-lobe complex was located in the abyssal plain with turbidite channels of different sizes developed (Figure 10). It is characterized by a long strip shape extending in the NE direction, diagonally to the continental shelf edge. In the study area, it has a distribution area of ~1600 km² with a length of up to 120 km (Figure 10). The turbidite channels show a U-shaped feature and flowed from the southwest to the northeast. They are marked by a high ratio of width to depth (average: 75) with an average erosion depth of less than 120 m (Figures 6–8).

Deepwater channel systems were located to the east of the submarine fan with Channels C1 and C2 developed (Figure 10). They are V-shaped on the seismic profiles with the characteristics of deep erosion depths (up to 250 m) (Figures 6–8). The flow direction of these channels is from southwest to northeast, but oblique to the extension direction of the submarine fan (Figure 10). Channel levees were developed on the right flanks of Channel C2. In addition, six phases of MTDs developed in the northern and southern of the study area, and two phases of slope fans were distributed only in the northern region (Figure 10).

Unit 2 sedimentary period: The distributary channel-lobe complex shared similar characteristics with Unit 1, but its range was greatly expanded to the region of Well 1 with a maximum width of up to 33 km (Figure 10). The distributary channel-lobe complex has a distribution region of ~2400 km² with a length of 135 km (Figure 10). Notably, the scale and distribution region of turbidite channels in this unit were considerably larger compared to Unit 1. Deepwater channel systems in Unit 2 displayed similarities with Unit 1, yet their distribution region overlapped with that of the submarine fan. During this period, five phases of MTDs and four phases of slope fans formed, and their distribution regions are smaller than the previous stage (Figure 10).

Unit 3 sedimentary period: Within this period, the distributary channel-lobe complex reached its largest size in the study area, covering a vast area of 2800 km² (Figure 11). The length and width

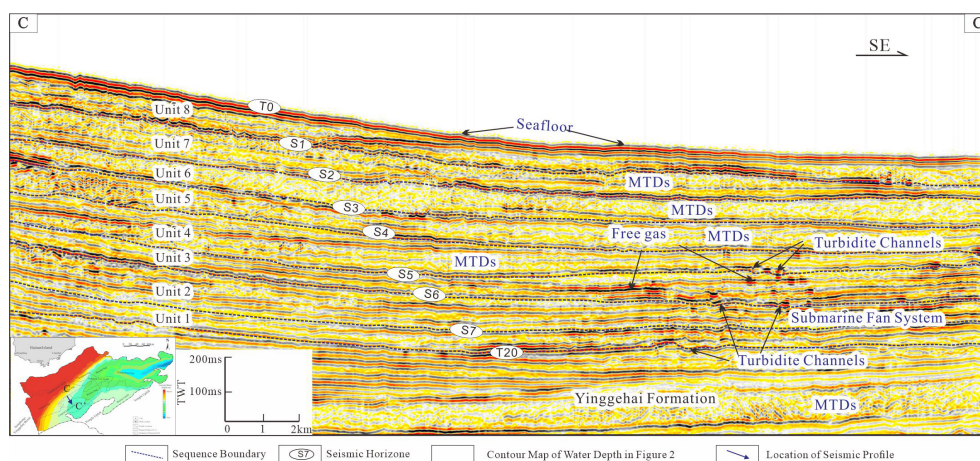


FIGURE 6

Interpreted seismic profile CC' crossed the submarine fan in the Qiongdongnan Basin, showing the sedimentary architecture of the submarine fan in the study area. The location of the seismic profile CC' is shown in Figure 3.

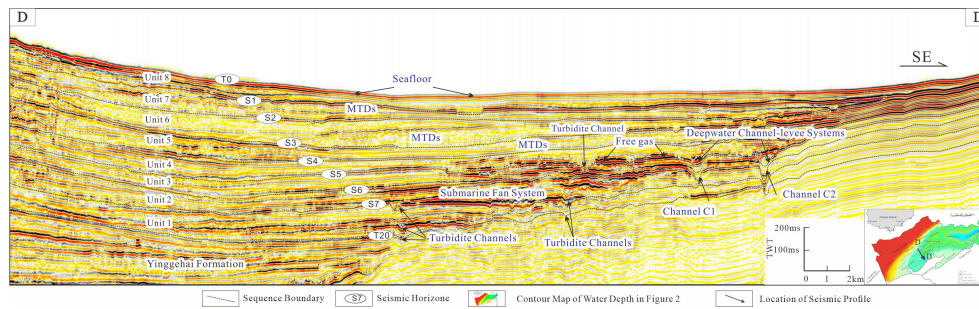


FIGURE 7

Interpreted seismic profile DD' crossed the submarine fan in the Qiongdongnan Basin, showing the sedimentary architecture of the submarine fan and the deepwater channel-levee systems in the study area. The location of the seismic profile DD' is shown in Figure 3.

of this complex expanded to 140 km and 35 km respectively (Figure 11). The turbidite channels were widespread to the south of Well 1. Deepwater channel systems continued to develop and primarily deposited pelagic sediments internally. While the channel levees were comparatively smaller, their number increased in comparison to previous stages. Similar to Unit 2, Unit 3 witnessed the formation of five phases of MTDs, yet their distribution regions were smaller than those of other stages (Figure 11).

This phase marked a notable shift in the sedimentary systems within the study area, as depicted in Figure 11. Several prominent transformations became evident during this period. Firstly, the extent of the submarine fan's depositional range witnessed a reduction, while deepwater channels experienced a notable expansion. Secondly, the emergence of Channel C3 became apparent, representing a significant development. Thirdly, the distributary channel-lobe complex displayed a division into two distinct sections: the northern and southern portions, illustrated in Figure 11. These segments respectively measure 75 km and 30 km in length, extending in a northeastern direction. The seismic profiles underscored the presence of turbidite channels within the submarine fan, characterized by profound erosion depths and

distinct "V" shapes. An intriguing observation within Unit 4 pertains to the remarkable depth of turbidite channel fills, reaching up to 160 m, a value considerably surpassing that of other units as depicted in Figures 6–8. Notably, in the eastern part of the study area, the geological formations underwent erosion from currents, leading to the formation of a novel Channel C3, as indicated in Figure 11. Differing from the preceding stages, this period exhibited a scarcity of channel levees. Additionally, a multitude of MTDs were widely distributed in the northern region, with their cumulative extent reaching a peak, as visually represented in Figure 11.

Unit 5 sedimentary period: The sedimentary dynamics during this phase depicted further contraction in the distribution range of the distributary channel-lobe complex, becoming confined to the vicinity surrounding Well 2, as illustrated in Figure 11. Within the study area, this complex covers an expanse of 200 km² (Figure 11). By contrast, the evolution of deepwater channel systems persisted, albeit accompanied by significant shifts in their distribution patterns. Channels C1 and C2 amalgamated in the southern region, while the progression of Channel C3 was notably absent (Figure 11). Similar to the previous Unit 4, multiple phases of MTDs were widely distributed in the study area (Figure 11).

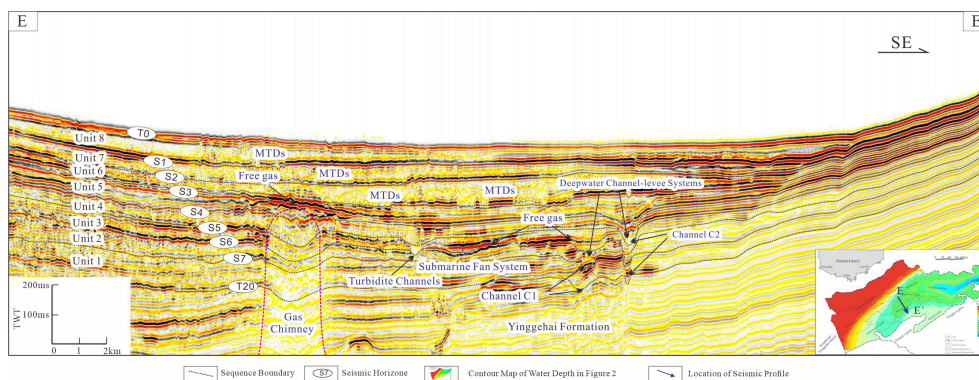


FIGURE 8

Interpreted seismic profile EE' crossed the submarine fan in the Qiongdongnan Basin, showing the sedimentary architecture of the submarine fan and the deepwater channel-levee systems in the study area. The location of the seismic profile EE' is shown in Figure 3.

5 Discussion

5.1 Sedimentary characteristics of the sand-rich submarine fan and its differences from the deepwater channel-levee systems

The deep oceans are predominantly composed of unconsolidated mudstone sediments during the Quaternary

period (Liu et al., 2016; Shen et al., 2023). Thus, searching for sandy deposits is particularly significant for gas hydrate and shallow gas exploration because they are favorable to forming gas hydrate and shallow gas reservoirs due to their high physical properties (Uchida and Tsuji, 2004; Collett et al., 2012; Portnova et al., 2019). Although sandy sediments have been reorganized in the deposits of deepwater channels within the Quaternary Ledong Formation of the Qiongdongnan Basin (Ren et al., 2022; Cheng et al., 2023), the

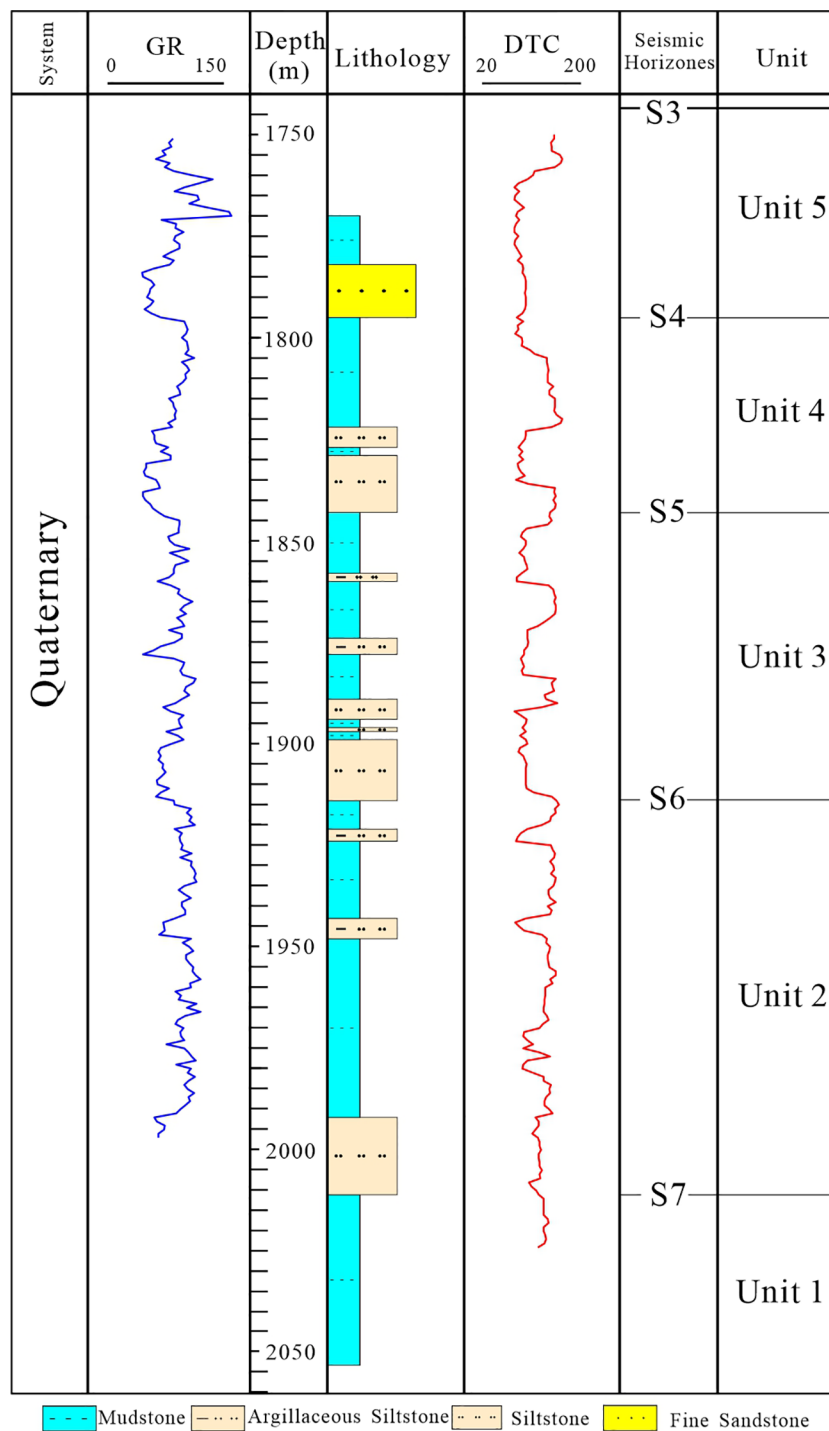
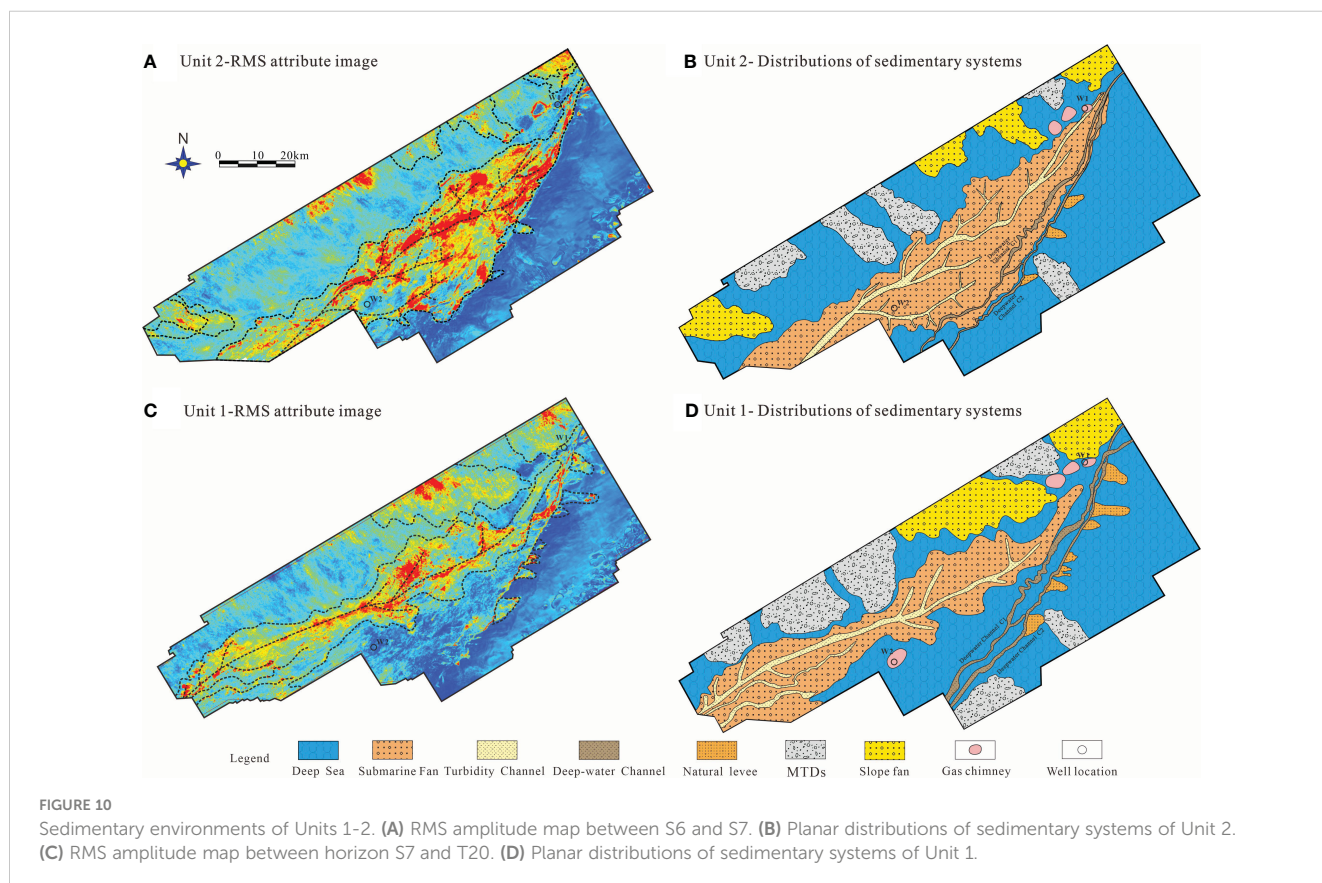


FIGURE 9 Stratigraphic column and well logging data of Well 2, showing the submarine fan is a sand-rich one. The location of Well 2 is shown in Figure 3.

scale of these sediments is extremely limited. In this study, we present evidence of a large-scale sand-rich submarine fan that encompasses multiple stages of siltstone to fine sandstone reservoirs (Figures 10, 11). With an area coverage reaching up to 2800 km² and a maximum thickness of 300 m (Figures 10, 11), this submarine fan provides a significant exploration opportunity for gas hydrate and shallow gas prospects within the Qiongdongnan Basin. The turbidite channels that filled in the submarine fan are composed of five stages of distributary channel-lobe complexes with a total thickness of sandstones up to 100 m (Figures 6–8, 12). Thus, this sand-rich submarine fan should be considered a novel exploration target for gas hydrate and shallow gas resources in the Qiongdongnan Basin.

In the abyssal plain, there are three types of depositional facies: deepwater channel-levee systems, submarine fans, and MTDs (Figures 10, 11). MTDs are readily identifiable in seismic profiles due to their characteristic large-scale chaotic reflection patterns (Wu et al., 2023) (Figures 6–8). However, differentiating between deepwater channel-levee systems and submarine fans can be challenging as they share common features, such as the presence of channels with erosion grooves (Figures 6–8). Previous studies by Cheng et al. (2023) and Ren et al. (2022) suggested the study area only developed deepwater channel-levee systems. However, our newly acquired comprehensive 3D seismic data and well data reveal the presence of both deepwater channel-levee systems and submarine fans with distinct depositional characteristics. Several lines of evidence support this conclusion. Firstly, the depositional

system exhibits a tongue shape with a maximum width of 35 km and an erosion depth of less than 150 m, significantly lower than that observed in the central canyon deposited during the Miocene Huangliu Formation (Figures 10, 11). These characteristics strongly indicate the presence of a large-scale submarine fan system. Secondly, the turbidite channels within the submarine fan display notable differences from the deepwater channels located on the right side of the submarine fan. The turbidite channels within the submarine fan system possess an average depth of 26 m and an average width-to-depth ratio of 75, whereas deepwater channels exhibit average depths of 83 m and width-to-depth ratios of 21 (Figures 6–8). Compared with turbidite channels, deepwater channels are characterized by higher erosion depth with “V” shapes, narrower channel width, and lower ratios of width to depth (Figures 6–8). Lastly, deepwater channel-levee systems are observed to have developed subsequent to the formation of the submarine fan, as evident from the reworking of submarine fan deposits by deepwater channels (Figures 6–8). These sedimentary distinctions between the submarine fan and deepwater channel-levee systems highlight the importance of conducting future exploration at various levels. In conclusion, this study demonstrates the presence of a significant sand-rich submarine fan in the Qiongdongnan Basin, which offers great potential for the exploration of gas hydrate and shallow gas resources. Additionally, our findings emphasize the need to distinguish between submarine fan and deepwater channel-levee systems, as they exhibit distinct sedimentary characteristics, ultimately guiding future exploration efforts.

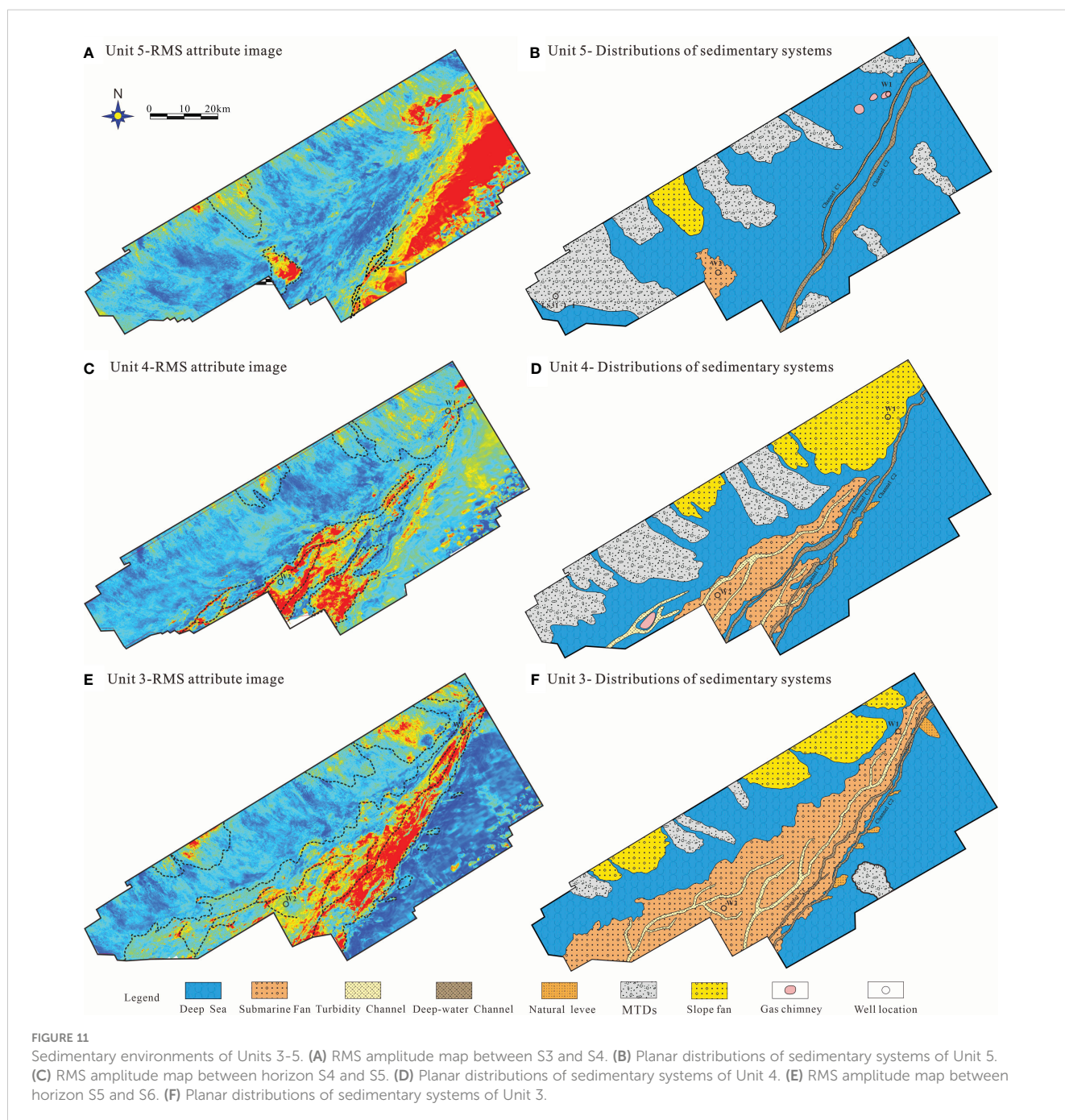


5.2 Major controlling factors for the evolution of the submarine fan

This study uncovers a five-stage evolution process of a single submarine fan system (Figures 10, 11). These stages are characterized by great variabilities in distribution range and stacking patterns. The distribution range gradually expanded from Unit 1 to Unit 3, followed by a rapid decrease during the sedimentary periods of Unit 4 and Unit 5 (Figures 10, 11). During this evolution process, the architecture of the submarine fan changed greatly, especially the locations of turbidite channel fills. Previous studies have attributed the formation and evolution of

submarine fans to various factors, including activities of synsedimentary faults, basement subsidence, geomorphology, sediment supply, and sea level changes (Mattern, 2005; Deptuck et al., 2008; Brooks et al., 2018). Furthermore, these controlling factors have been found to vary across different depositional settings (Mattern, 2005; Deptuck et al., 2008). Based on our findings, we suggest that the evolution of the sand-rich submarine fan in this study is closely linked to fluctuations in sea level, sediment supply, and geomorphology.

Sea level fluctuation plays a significant role in shaping submarine fan development (Normark et al., 1998; Richard et al., 1998; Covault et al., 2007; Zhang et al., 2018). Extensive research has



been conducted on relative sea level fluctuation in the northern China Sea (Haq et al., 1987; Miller et al., 2005; Shao et al., 2017). Although there are discrepancies in sea level curves due to resolution differences, all reported curves exhibit a pronounced declining trend during the sedimentary period of Units 1-3 and a significant rising trend during the sedimentary period of Units 4-5 (Figure 12). During periods of sea level fall, terrigenous sediments are readily transported along submarine slopes into abyssal plains, giving rise to large-scale submarine fan systems (Normark et al., 1998; Zhang et al., 2018). Conversely, sea level rise periods typically result in lower sediment supplies, leading to a lack of sediment influx. This is consistent with the evolution history that the distribution range of the submarine fan gradually increased from Unit 1 to Unit 3 and then decreased from Unit 4 to Unit 5 (Figures 10, 11). Thus, the lower stratigraphic interval (Unit 1 to Unit 3) is interpreted to represent the lowstand systems tract (LST) that formed during the sea-level rapidly fell period, while the upper stratigraphic interval (Unit 4 to Unit 5) should correspond to transgressive systems tract (TST) (Figure 12).

It is worth noting that the submarine fan in this study exhibits a tongue-shaped morphology, which significantly differs from commonly developed fan shapes, indicating it is a typical confined fan. Previous studies have found a strong correlation between submarine fan shape and the degree of confinement in geomorphology (Sinclair and Cowie, 2003; Hou et al., 2022). As the degree of confinement in geomorphology increases, the corresponding submarine fan demonstrates a reduced lateral width and an extended longitudinal length, gradually

transitioning from a fan-shaped to a tongue-shaped planar evolution (Liu et al., 2014; Zhang et al., 2016). The palaeogeographic map as well as seismic profiles show that the submarine fan was deposited in a setting with a confined tectonic trough. The sediments transported by slope-channel systems filled the confined trough, with the distribution direction of the submarine fan the same as the extension direction of the confined trough (Figure 13). Similar settings have also been documented in the Adana Basin, southern Turkey, and Messinian Laga Basin, Italy (Satur et al., 2004; Marini et al., 2015). Hence, we propose that confined geomorphology is another significant controlling factor in submarine fan development. The confined trough in the abyssal plain provided ample accumulation space for sediments transported by slope-channel systems, ultimately leading to the tongue-shaped morphology of the submarine fan (Figure 13).

Apart from sea level fluctuation and confined geomorphology, sediment supply is also a crucial factor in the occurrence of this large-scale sand-rich submarine fan. Previous studies have suggested that the Qiongdongnan Basin has a complex source-to-sink system, with the Red River, Truong Son Belt, Taiwan Island, and Hainan Island serving as potential source areas (Cheng et al., 2022; Liu et al., 2022; Huang et al., 2023). Cheng et al. (2022) reported the zircon U-Pb data of the Ledong Formation sediments in the Qiongdongnan Basin, suggesting that the Red River and Truong Son Belt are the primary sources. Considering that the Red River is located at least 700 km away from the submarine fan (Figure 1), sediments originating from the Red River exhibit a high mud content but low sandy content. By contrast, the proximity of

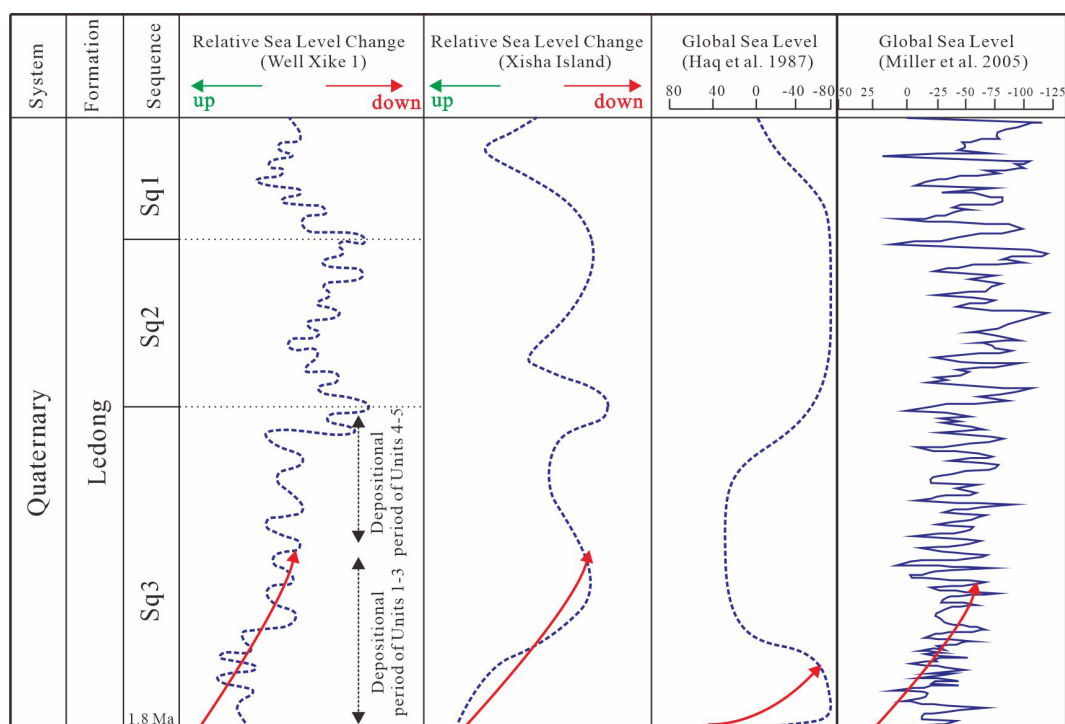


FIGURE 12

Sea level changes during the sedimentary period of the Quaternary Ledong Formation. The sea level curves are from Haq et al. (1987); Miller et al. (2005), and Shao et al. (2017).

the Truong Son Belt, only 150 km from the depocenter, allows for the transport of sandy sediments to the Qiongdongnan Basin's central region. Additionally, there are numerous rivers in the surrounding area of the Truong Son Belt that carry significant sediment loads into the South China Sea each year (Milliman and Farnsworth, 2013). Huang et al. (2023) suggests that the Taiwan Island also have significant contributions to the Qiongdongnan Basin with the deep-water current and shallower Kuroshio Current being the main transport pathways. Hainan Island is also considered a source area, but its contribution is less than 20% due to minimal denudation (Cheng et al., 2022). Under the combined action of turbidity currents and surface currents, the sediments from the Red River and Truong Son Belt can be further mixed with the sediments from Hainan Island transported by the continental slope-channel systems and finally deposited in the confined trough in the abyssal plain (Figure 13). Meanwhile, the deep-water current and shallower Kuroshio Current can transport the sediments from the Taiwan Island to the confined trough in the abyssal plain towards the southwest (Figure 13). But the main routes for sediments transportation as well as the contribution of each provenance area need to be further investigated.

5.3 Implications for gas hydrate and shallow gas exploration

Qiongdongnan Basin holds significant importance as a hydrocarbon-rich region within the South China Sea. Historically, exploration efforts were predominantly concentrated on tapping into the deep-buried reservoirs (Gong et al., 2011; Huang et al., 2016). Recent studies, however, have unearthed substantial gas hydrate and shallow gas resources within the shallower strata, indicating immense resource potential (Meng et al., 2022; Ren et al., 2022; Cheng et al., 2023). Shallow gas plays a crucial role as a conventional natural gas resource in strata less than 1000 m. In the past century, significant progress has been made in its exploitation, leading to a breakthrough in commercial exploration (Verweij et al., 2018; Zou et al., 2023). On the other hand, gas hydrate is still in the

stage of production testing, calling for more focus on shallow gas exploration (Boswell and Collett, 2011; Zou et al., 2023). The Dutch part of the Southern North Sea Delta, for instance, has established five shallow gas fields with a total volume of 118 billion cubic meters of Gas Initially In Place (Verweij et al., 2018). Nonetheless, exploring these gas hydrate and shallow gas reservoirs comes with substantial challenges, mainly due to the scarcity of high-quality reservoirs. Apart from its importance in the petroleum industry, comprehending the shallow gas system is vital for assessing marine geohazards since the leakage of shallow gas can lead to significant dangers in the marine environment.

In recent times, exploration endeavors aimed at uncovering gas hydrate and shallow gas have predominantly focused on the intricacies of deepwater channel-levee systems (Meng et al., 2022; Ren et al., 2022; Cheng et al., 2023). An illustrative instance is the drilling of deepwater channel fills in Well W1 in 2019 (Meng et al., 2021; Xu et al., 2021), revealing multiple layers of gas hydrate and shallow gas reservoirs. Notably, the development scale of these deepwater channel fills is relatively limited, spanning less than 1.0 km in width. In contrast, the current study identifies a submarine fan of substantial dimensions, covering a sprawling 2800 km² area, with a maximum length and width of 140 km and 35 km, respectively (Figure 11). The turbidite channels within the submarine fan have an average width of 1.5 km, significantly wider than the deepwater channels. Moreover, it is worth noting that the size and quantity of turbidite channels are larger than that of deepwater channels. The turbidite channel fills represent extremely strong amplitude anomalies in the RMS attribute images, suggesting they are sand-rich sediments. This assertion is reinforced by log interpretation results from Well 2 (Figure 9), where the turbidite channel fills showcase porosity levels ranging from 39% to 44%, averaging at 41%, surpassing the underlying Yinggehai Formation reservoirs (Liu et al., 2023). Conversely, the deepwater channels exhibit relatively subdued amplitude features, hinting at muddier sediments with lower sand content. Thus, when juxtaposed against the earlier exploration targets (deepwater channels), the submarine fan, particularly its turbidite channel fills, boasts a more expansive developmental scale, superior

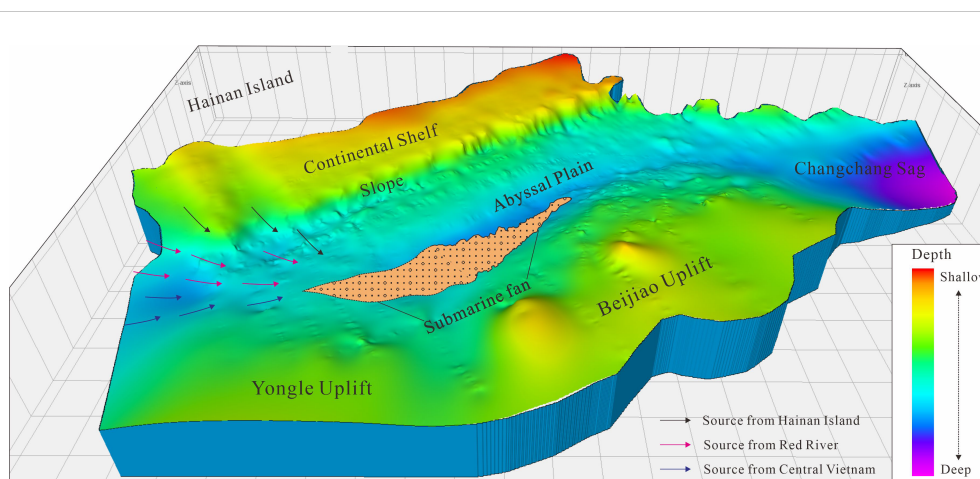


FIGURE 13

The palaeogeographic map of Horizon T20, showing the submarine fan was located in a confined geomorphology.

reservoir properties, and heightened exploration potential. This positions the turbidite channel fills within the submarine fan as pivotal prospects for forthcoming gas hydrate and shallow gas exploration endeavors. Turbidite channels nested within submarine fans hold promising potential for engendering large-scale lithologic traps (Cui et al., 2021; Liu et al., 2021).

Turbidite channels within submarine fans have great potential to form large-scale lithologic traps (Cui et al., 2021; Liu et al., 2021). In the Qiongdongnan Basin, deep thermogenic gas and microbial methane migrated vertically to the Quaternary Ledong Formation through gas chimneys or sedimentary faults (Lai et al., 2021). Simultaneously, multiple-stage MTDs deposits in Units 5–7 acted as good seals for hydrocarbon accumulation, blocking the leakage of shallow gas. Large quantities of free gas accumulated in the underlying strata of Units 1–4 (Figures 10, 11). Benefitting from favorable reservoir properties, shallow gas reservoirs subsequently materialized within the turbidite channels of the submarine fan system, with the potential for gas hydrate reservoirs to form in upper gas chimneys under suitable temperature and pressure conditions (Yuan et al., 2021). Noteworthy findings from exploration in Well 2 underscore the Qiongdongnan Basin's submarine fan system as a repository of abundant shallow gas resources and conducive conditions for gas accumulation. Consequently, both the turbidite channels within the submarine fan and deepwater channels emerge as promising targets for offshore shallow gas exploration within the shallow strata of the Qiongdongnan Basin.

6 Conclusions

(1) This study utilizes newly acquired 3D seismic data and well data to characterize a sand-rich submarine fan situated in the abyssal plain of the Qiongdongnan Basin, South China Sea, at depths ranging from 1300 to 1700 m. This deep-water fan exhibits a distinctive tongue-shaped configuration in the plane, oriented in a southwest to northeast direction, which differs from the commonly observed fan shapes. Its lithology is primarily composed of unconsolidated silty clays interbedded with layers of sand.

(2) The submarine fan consists of five stages of distributary channel-lobe complexes, the distribution ranges of which gradually increased from Unit 1 to Unit 3 and then decreased from Unit 4 to Unit 5. Among them, Unit 3 occupies the largest area of ~2800 km² with its length and width reaching 140 km and 35 km, respectively.

(3) The formation and evolution of this submarine fan are primarily governed by sea level fluctuation, confined geomorphology, and sediment supply. The sediments derived from Red River, Truong Son Belt, Taiwan Island, and Hainan Island were transported by the continental slope-channel systems and ocean currents and finally deposited in the confined trough in the abyssal plain. This process has given rise to this extensive sand-rich submarine fan system. The distribution of distributary channel-lobe complexes expanded during periods of falling sea levels but contracted during periods of rising sea levels.

(4) There exist notable disparities in sedimentary characteristics between the submarine fan and deepwater channel-levee systems. Deepwater channels within deepwater channel-levee systems are

distinguished by their substantial erosion depth, V-shaped profiles, and low width-to-depth ratio. Conversely, the distributary turbidite channels within the submarine fan exhibit shallower erosion depths, U-shaped profiles, greater channel widths, and higher width-to-depth ratios. The turbidite channels represent the most significant targets for offshore shallow gas exploration in the Qiongdongnan Basin due to their extensive developmental scale and favorable reservoir physical properties.

Data availability statement

The original contributions presented in the study are included in the article/supplementary material. Further inquiries can be directed to the corresponding authors.

Author contributions

EL: Conceptualization, Data curation, Investigation, Writing – original draft. DY: Funding acquisition, Supervision, Writing – review & editing. XL: Data curation, Methodology, Software, Writing – original draft. JP: Resources, Writing – review & editing. JZ: Formal analysis, Methodology, Software, Writing – original draft.

Funding

The author(s) declare financial support was received for the research, authorship, and/or publication of this article. This work was supported by the National Natural Science Foundation of China (Nos. 42072142, 41702121 and U19B2007).

Acknowledgments

We gratefully acknowledge the editor for careful editorial handling and the two reviewers for reviewing this manuscript.

Conflict of interest

Author JP is employed by China National Offshore Oil Corporation.

The remaining authors declare that the research was conducted in the absence of any commercial or financial relationships that could be construed as a potential conflict of interest.

Publisher's note

All claims expressed in this article are solely those of the authors and do not necessarily represent those of their affiliated organizations, or those of the publisher, the editors and the reviewers. Any product that may be evaluated in this article, or claim that may be made by its manufacturer, is not guaranteed or endorsed by the publisher.

References

- Boswell, R., and Collett, T. S. (2011). Current perspectives on gas hydrate resources. *Energy Environ. Sci.* 4, 1206–1215. doi: 10.1039/c0ee00203h
- Boswell, R., Sheldner, D., Lee, M., Latham, T., Collett, T., Guerin, G., et al. (2009). Occurrence of gas hydrate in Oligocene Frio sand: Alaminos canyon block 818: northern Gulf of Mexico. *Mar. Petrol. Geol.* 26, 1499–1512. doi: 10.1016/j.marpetgeo.2009.03.005
- Brooks, H. L., Hodgson, D. M., Brunt, R. L., Peakall, J., Hofstra, M., and Flint, S. S. (2018). Deep-water channel-lobe transition zone dynamics: processes and depositional architecture, an example from the Karoo Basin, South Africa. *Geol. Soc. Am. Bull.* 130, 1723–1746. doi: 10.1130/B31714.1
- Catuneanu, O., and Zecchin, M. (2016). Unique vs. non-unique stratal geometries: Relevance to sequence stratigraphy. *Mar. Pet. Geol.* 78, 184–195. doi: 10.1016/j.marpetgeo.2016.09.019
- Chen, W., Wu, S., Wang, D., Betzler, C., and Ma, Y. (2023). Stratigraphic evolution and drowning steps of a submerged isolated carbonate platform in the northern South China Sea. *Front. Mar. Sci.* 10. doi: 10.3389/fmars.2023.1200788
- Cheng, C., Jiang, T., Kuang, Z., Lai, H., Liang, J., Ren, J., et al. (2023). Sand-rich Pleistocene deep-water channels and their implications for gas hydrate accumulation: Evidence from the Qiongdongnan Basin, northern South China Sea. *Deep-Sea Res. Part I* 198, 104101. doi: 10.1016/j.dsr.2023.104101
- Cheng, C., Kuang, Z., Jiang, T., Cao, L., Ren, J., Liang, J., et al. (2022). Source of the sand-rich gas hydrate reservoir in the northern South China Sea: insights from detrital zircon U-Pb geochronology and seismic geomorphology. *Mar. Petrol. Geol.* 145, 105904. doi: 10.1016/j.marpetgeo.2022.105904
- Clift, P. D., and Gaedicke, C. (2002). Accelerated mass flux to the Arabian Sea during the middle to late Miocene. *Geology* 30, 207–210. doi: 10.1130/0091-7613(2002)030<0207:AMFTTA>2.0.CO;2
- Clift, P. D., and Sun, Z. (2006). The sedimentary and tectonic evolution of the Yinggehai-Song Hong basin and the southern Hainan margin, South China Sea: implications for Tibetan uplift and monsoon intensification. *J. Geophys. Res. Solid Earth* 111, B6. doi: 10.1029/2005JB004048
- Collett, T. S., Lee, M. W., Zyrianova, M. V., Mrozewski, S. A., Guerin, G., Cook, A. E., et al. (2012). Gulf of Mexico gas hydrate joint industry project leg II logging-while-drilling data acquisition and analysis. *Mar. Pet. Geol.* 34, 41–61. doi: 10.1016/j.marpetgeo.2011.08.003
- Covault, J. A., Normark, W. R., Romans, B. W., and Graham, S. A. (2007). Highstand fans in the California borderland: The overlooked deep-water depositional systems. *Geology* 35 (9), 783–786. doi: 10.1130/G23800A.1
- Cui, J. W., Yuan, X. J., Wu, S. T., Zhang, R. F., Jin, S., and Li, Y. (2021). Rock types and reservoir characteristics of Shahejie Formation Marl in Shulu Sag, Jizhong Depression, Bohai Bay Basin. *J. Earth Sci.* 32 (4), 986–997. doi: 10.1007/s12583-020-1092-5
- Deptuck, M. E., Piper, D. J. W., Savoye, B., and Gervais, A. (2008). Dimensions and architecture of late Pleistocene submarine lobes off the northern margin of east Corsica. *Sedimentology* 55, 869–898. doi: 10.1111/j.1365-3091.2007.00926.x
- Fyhn, M. B. W., Thomsen, T. B., Keulen, N., Knudsen, C., Rizzi, M., Bojesen-Koefoed, J., et al. (2019). Detrital zircon ages and heavy mineral composition along the Gulf of Tonkin - implication for sand provenance in the Yinggehai-Song Hong and Qiongdongnan basins. *Mar. Petrol. Geol.* 101, 162–179. doi: 10.1016/j.marpetgeo.2018.11.051
- Gong, C., Qi, K., Ma, Y., Li, D., and Xu, H. (2019). Tight coupling between the cyclicity of deep-water systems and rising-then-flat shelf-edge pairs along the submarine segment of the Qiongdongnan sediment-routing system. *J. Sediment. Res.* 89 (10), 956–975. doi: 10.2110/jsr.2019.47
- Gong, C., Wang, Y., Zhu, W., Li, W., Xu, Q., and Zhang, J. (2011). The central submarine canyon in the Qiongdongnan Basin, northwestern south China Sea: architecture, sequence stratigraphy, and depositional processes. *Mar. Petrol. Geol.* 28, 1690–1702. doi: 10.1016/j.marpetgeo.2011.06.005
- Haq, B. U., Hardenbol, J. A. N., and Vail, P. R. (1987). Chronology of fluctuating sea levels since the Triassic. *Science* 235, 1156–1167. doi: 10.1126/science.235.4793.1156
- Hawie, N., Covault, J. A., and Sylvester, Z. (2019). Grain-size and discharge controls on submarine-fan depositional patterns from forward stratigraphic models. *Front. Earth Sci.* 7. doi: 10.3389/feart.2019.00334
- Horozal, S., Lee, G. H., Yi, B. Y., Yoo, D. G., Park, K. P., Lee, H. Y., et al. (2009). Seismic indicators of gas hydrate and associated gas in the Ulleung Basin, East Sea (Japan Sea) and implications of heat flows derived from depths of the bottom-simulating reflector. *Mar. Geol.* 258, 126–138. doi: 10.1016/j.marpetgeo.2008.12.004
- Hou, P. F., Jobe, Z. R., and Wood, L. J. (2022). Statistical characterization of a confined submarine fan system: The Pennsylvanian Lower Atoka Formation, Ouachita Mountains, USA. *Sedimentology* 69, 775–797. doi: 10.1111/sed.12925
- Huang, B., Tian, H., Li, X., Wang, Z., and Xiao, X. (2016). Geochemistry, origin and accumulation of natural gases in the deepwater area of the Qiongdongnan Basin, South China Sea. *Mar. Petrol. Geol.* 72, 254–267. doi: 10.1016/j.marpetgeo.2016.02.007
- Huang, Q. T., Hua, Y. J., Zhang, C. L., Cheng, P., Wan, Z. F., Hong, T., et al. (2023). Provenance and transport mechanism of gravity core sediments in the deep-water area of the Qiongdongnan Basin, northern South China Sea. *Mar. Geol.* 459, 107043. doi: 10.1016/j.marpetgeo.2023.107043
- Lai, H. F., Fang, Y. X., Kuang, Z. G., Ren, J. F., Liang, J. Q., Lu, J. A., et al. (2021). Geochemistry, origin and accumulation of natural gas hydrates in the Qiongdongnan Basin, South China Sea: implications from site GMGS5-W08. *Mar. Petrol. Geol.* 123, 104774. doi: 10.1016/j.marpetgeo.2020.104774
- Li, Q., Zhong, G., and Tian, J. (2009). "Stratigraphy and sea level changes," in *The South China Sea: Paleocyanography and Sedimentology*. Eds. P. Wang and Q. Li (Netherlands, Dordrecht: Springer), 75–170.
- Liu, E. T., Chen, S., Yan, D. T., Deng, Y., Wang, H., Jing, Z. H., et al. (2022). Detrital zircon geochronology and heavy mineral composition constraints on provenance evolution in the western Pearl River Mouth basin, northern south China sea: A source to sink approach. *Mar. Petrol. Geol.* 145, 105884. doi: 10.1016/j.marpetgeo.2022.105884
- Liu, K., Cheng, P., Tian, H., Song, P., and Hu, W. (2023). Development model of shallow lithologic traps and natural gas accumulation mechanisms in marine deep-water areas: A case study in the Qiongdongnan basin, south China sea. *Mar. Petrol. Geol.* 151, 106211. doi: 10.1016/j.marpetgeo.2023.106211
- Liu, E. T., Wang, H., Feng, Y. X., Pan, S. Q., Jing, Z. H., Ma, Q. L., et al. (2020). Sedimentary architecture and provenance analysis of a sublacustrine fan system in a half-graben rift depression of the South China Sea. *Sediment. Geol.* 409, 105781. doi: 10.1016/j.sedgeo.2020.105781
- Liu, E. T., Wang, H., Li, Y., Zhou, W., Nicole, D. L., Lin, Z. L., et al. (2014). Sedimentary characteristics and tectonic setting of sublacustrine fans in a half-graben rift depression, Beibuwan Basin, South China Sea. *Mar. Petrol. Geol.* 52, 9–21. doi: 10.1016/j.marpetgeo.2014.01.008
- Liu, E. T., Wang, H., Pan, S. Q., Qin, C. Y., Jiang, P., Chen, S., et al. (2021). Architecture and depositional processes of sublacustrine fan systems in structurally active settings: An example from Weixian Depression, northern South China Sea. *Mar. Petrol. Geol.* 134, 105380. doi: 10.1016/j.marpetgeo.2021.105380
- Liu, Z., Zhao, Y., Colin, C., Statteger, K., Wiesner, M. G., Huh, C.-A., et al. (2016). Source-to-sink processes of fluvial sediments in the South China Sea. *Earth-Sci. Rev.* 153, 238–273. doi: 10.1016/j.earscirev.2015.08.005
- Marini, M., Milli, S., Ravnas, R., and Moscatelli, M. (2015). A comparative study of confined vs. semi-confined turbidite lobes from the Lower Messinian Laga Basin (Central Apennines, Italy): Implications for assessment of reservoir architecture. *Mar. Pet. Geol.* 63, 142–165. doi: 10.1016/j.marpetgeo.2015.02.015
- Mattern, F. (2005). Ancient sand-rich submarine fans: depositional systems, models, identification, and analysis. *Earth-Sci. Rev.* 70, 167–202. doi: 10.1016/j.earscirev.2004.12.001
- Meng, M., Liang, J., Kuang, Z., Ren, J., He, Y., Deng, W., et al. (2022). Distribution characteristics of quaternary channel systems and their controlling factors in the Qiongdongnan Basin, south China sea. *Front. Earth Sci.* 10. doi: 10.3389/feart.2022.902517
- Meng, M., Liang, J., Lu, J. A., Zhang, W., Kuang, Z., Fang, Y., et al. (2021). Quaternary deep-water sedimentary characteristics and their relationship with the gas hydrate accumulations in the Qiongdongnan Basin, Northwest South China Sea. *Deep. Sea Res. Part I* 177, 103628. doi: 10.1016/j.dsr.2021.103628
- Miller, K. G., Komins, M. A., Browning, J. V., Wright, J. D., Mountain, G. S., Katz, M. E., et al. (2005). The Phanerozoic record of global sea-level change. *Science* 310, 1293–1298. doi: 10.1126/science.1116412
- Milliman, J. D., and Farnsworth, K. L. (2013). *River discharge to the coastal ocean: A global synthesis* (Cambridge: Cambridge University Press).
- Normark, W. R. (1970). Growth patterns of deep-sea fans. *AAPG. Bull.* 54, 2170–2195. doi: 10.1306/5D25CC79-16C1-11D7-8645000102C1865D
- Normark, W. R., Piper, D. J. W., and Hiscott, R. N. (1998). Sea level controls on the textural characteristics and depositional architecture of the Hueneme and associated submarine fan systems, Santa Monica Basin, California. *Sedimentology* 45, 53–70. doi: 10.1046/j.1365-3091.1998.00139.x
- Pickering, K. T., Corregidor, J., and Clark, J. D. (2015). Architecture and stacking patterns of lower-slope and proximal basin-floor channelised submarine fans, Middle Eocene Ainsa System, Spanish Pyrenees: An integrated outcrop-subsurface study. *Earth-Sci. Rev.* 144, 47–81. doi: 10.1016/j.earscirev.2014.11.017
- Piper, D. J., and Normark, W. R. (2001). Sandy fans from Amazon to Hueneme and beyond. *AAPG. Bull.* 85, 1407–1438. doi: 10.1306/8626CACD-173B-11D7-8645000102C1865D
- Portnova, A., Cooka, A. E., Sawyera, D. E., Yang, C., Hillman, J. I. T., and Waite, W. F. (2019). Clustered BSRs: Evidence for gas hydrate-bearing turbidite complexes in folded regions, example from the Perdido Fold Belt, northern Gulf of Mexico. *Earth Planet. Sci. Lett.* 528, 115843. doi: 10.1016/j.epsl.2019.115843
- Ren, J., Cheng, C., Xiong, P., Kuang, Z., Liang, J., Lai, H., et al. (2022). Sand-rich gas hydrate and shallow gas systems in the Qiongdongnan Basin, northern South China Sea. *J. Pet. Sci. Eng.* 215, 110630. doi: 10.1016/j.petrol.2022.110630

- Ren, J., Zhang, D., Tong, D., Huang, A., Wang, Y., Lei, C., et al. (2014). Characterising the nature, evolution and origin of detachment fault in central depression belt, Qiongdongnan Basin of South China Sea: evidence from seismic reflection data. *Acta Oceanol. Sin.* 33, 118–126. doi: 10.1007/s13131-014-0581-8
- Richard, M., Bowman, M., and Reading, H. (1998). Submarine-fan systems: i: characterization and stratigraphic prediction. *Mar. Pet. Geol.* 15 (7), 689–717. doi: 10.1016/S0264-8172(98)00036-1
- Samuel, A., Kneller, B., Raslan, S., Sharp, A., and Parsons, C. (2003). Prolific deep-marine slope channels of the Nile Delta, Egypt. *AAPG. Bull.* 87, 541–560. doi: 10.1306/1105021094
- Satur, N., Cronin, B., Hurst, A., Kelling, G., and Gürbüz, K. (2004). Downchannel variations in stratal patterns within a conglomeratic, deepwater fan feeder system (Miocene, Adana Basin, Southern Turkey). In: Lomas, S.A., and Joseph, P. (eds) Confined turbidite systems. *Geol. Soc. Lond. Spec. Publ.* 222, 241–260. doi: 10.1144/GSL.SP.2004.222.01.13
- Shao, L., Cui, Y. C., Qiao, P. J., Zhang, D. J., Liu, X. Y., and Zhang, C. L. (2017). Sea-level changes and carbonate platform evolution of the Xisha Islands (South China Sea) since the Early Miocene. *Palaeogeogr. Palaeoclimatol. Palaeoecol.* 485, 504–516. doi: 10.1016/j.palaeo.2017.07.006
- Shen, A., Sun, Q. L., Cai, D. Z., and Xing, Z. H. (2023). Characteristics, classification and genetic mechanism of pockmarks. *Bull. Geol. Sci. Technol.* 42 (1), 204–217. doi: 10.19509/j.cnki.dzkq.2022.0144
- Sinclair, H. D., and Cowie, P. A. (2003). Basin-floor topography and the scaling of turbidites. *J. Geol.* 111, 277–299. doi: 10.1086/373969
- Somme, T. O., Helland-Hansen, W., Martinsen, O. J., and Thurmond, J. B. (2009). Relationship between morphological and sedimentological parameters in source-to-sink systems: a basis for predicting semi-quantitative characteristics in subsurface systems. *Basin. Res.* 21, 361–387. doi: 10.1111/j.1365-2117.2009.00397.x
- Sun, Q. L., Wang, Q., Shi, F. Y., Alves, T., Gao, S., Xie, X. N., et al. (2022). Runup of landslide-generated tsunamis controlled by paleogeography and sea-level change. *Commun. Earth Environ.* 3, 244. doi: 10.1038/s43247-022-00572-w
- Talling, P. J., Wynn, R. B., Masson, D. G., Frenz, M., Cronin, B. T., Schiebel, R., et al. (2007). Onset of submarine debris flow deposition far from original giant landslide. *Nature* 450, 541–544. doi: 10.1038/nature06313
- Uchida, T., and Tsuji, T. (2004). Petrophysical properties of natural gas hydrates-bearing sands and their sedimentology in the Nankai Trough. *Resour. Geol.* 54, 79–87. doi: 10.1111/j.1751-3928.2004.tb00189.x
- Verweij, J. M., Nelskamp, S. N., Ten Veen, J. H., De Bruin, G., Geel, K., and Donders, T. H. (2018). Generation, migration, entrapment and leakage of microbial gas in the Dutch part of the Southern North Sea Delta. *Mar. Pet. Geol.* 97, 493–516. doi: 10.1016/j.marpetgeo.2018.07.034
- Wang, X. G., Zhang, H., Chen, Z. H., Tian, D. M., Li, W. R., Zhang, D. Y., et al. (2021). Numerical simulation of sedimentation in the Central Canyon of Lingshui area, Qiongdongnan Basin. *Bull. Geol. Sci. Technol.* 40 (5), 42–53. doi: 10.19509/j.cnki.dzkq.2021.0026
- Wu, N., Jackson, C. A. L., Clare, M. A., Hodgson, D. M., Nugraha, H., Steventon, M. J., et al. (2023). Diagenetic priming of submarine landslides in ooze-rich substrates. *Geology* 51, 85–90. doi: 10.1130/G50458.1
- Xiong, P. F., Jiang, T., Kuang, Z. G., Cheng, C., Ren, J. F., and Lai, H. F. (2021). Sedimentary characteristics and origin of mounds in Meishan Formation, southern Qiongdongnan Basin. *Bull. Geol. Sci. Technol.* 40 (4), 11–21. doi: 10.19509/j.cnki.dzkq.2021.0427
- Xu, L., Shi, K., Lv, X., Wei, R., Fan, Q., Li, Q., et al. (2021). Enhanced gas production from hydrate reservoirs with underlying water layer. *Energy Fuels.* 35, 1347–1357. doi: 10.1021/acs.energyfuels.0c03677
- Yuan, H. M., Wang, Y., and Wang, X. C. (2021). Seismic methods for exploration and exploitation of gas hydrate. *J. Earth Sci.* 32 (4), 839–849. doi: 10.1007/s12583-021-1502-3
- Yuan, S., Wu, S., Thomas, L., Yao, G., Lv, F., Cao, F., et al. (2009). Fine-grained Pleistocene deepwater turbidite channel system on the slope of Qiongdongnan Basin, northern South China Sea. *Mar. Petrol. Geol.* 26 (8), 1441–1451. doi: 10.1016/j.marpetgeo.2009.03.007
- Zeng, H. L. (2013). Frequency-dependent seismic-stratigraphic and facies interpretation. *AAPG. Bull.* 97 (2), 201–221. doi: 10.1306/06011212029
- Zhang, C., and Hou, J. (2022). Creep characteristics of muddy submarine channel slope instability. *Front. Mar. Sci.* 9. doi: 10.3389/fmars.2022.999151
- Zhang, J. J., Wu, S. H., Fan, T. E., Fan, H. J., Jiang, L., Chen, C., et al. (2016). Research on the architecture of submarine-fan lobes in the Niger Delta Basin, offshore West Africa. *J. Palaeogeogr.* 5 (3), 185–204. doi: 10.1016/j.jop.2016.05.005
- Zhang, J. J., Wu, S. H., Hu, G. Y., Fan, T. E., Yu, B., Lin, P., et al. (2018). Sea-level control on the submarine fan architecture in a deepwater sequence of the Niger Delta Basin. *Mar. Petrol. Geol.* 94, 179–197. doi: 10.1016/j.marpetgeo.2018.04.002
- Zhao, Z., Sun, Z., Sun, L., Wang, Z., and Sun, Z. (2016). Cenozoic tectonic subsidence in the Qiongdongnan Basin, northern South China Sea. *Basin Res.* 30, 269–288. doi: 10.1111/bre.12220
- Zou, C. N., Yang, Z., Zhang, G. S., Zhu, R. K., Tao, S. Z., Yuan, X. J., et al. (2023). Theory, technology and practice of unconventional petroleum geology. *J. Earth Sci.* 34 (4), 951–965. doi: 10.1007/s12583-023-2000-8